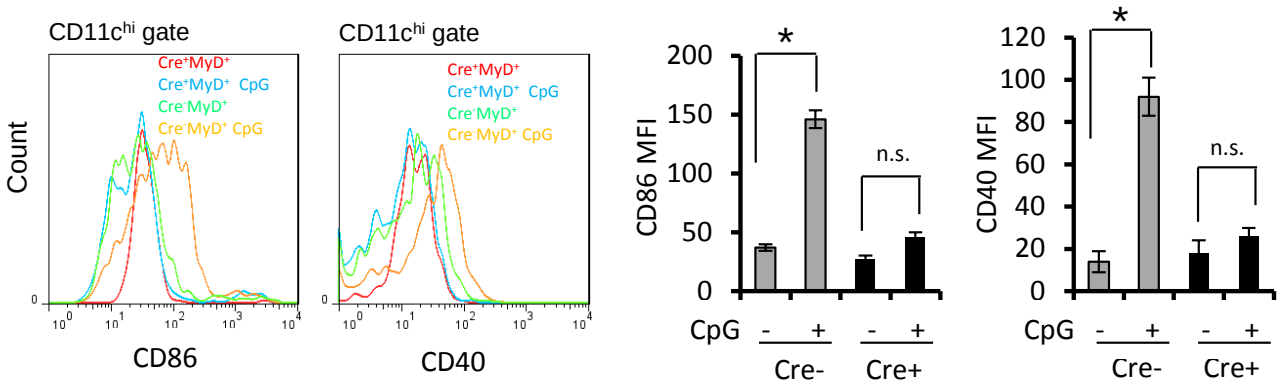

Supplementary Figure 1

***Cd11cCre^{+}MyD88$^{fl/fl}$* mice have defective splenic DC maturation.** Splenocytes were harvested from *Cd11cCre^{-}MyD88$^{fl/fl}$* and *Cd11cCre^{+}MyD88$^{fl/fl}$* mice 18 h after injection of 25 µg of CpG (orange and blue lines, respectively) or vehicle control (green and red lines respectively). Note that the CpG was complexed to a cationic lipid, 1,2-dioleoyloxy-3-trimethylammonium-propane-methylsulfate (DOTAP); control mice were injected with vehicle containing DOTAP without CpG. The histogram shows the cell surface expression levels of the DC maturation markers CD86 and CD40 on CD11c^{hi}- gated splenocytes from the indicated mice. The quantitative data from 3 mice per group is shown in the bar graphs. *, $p<0.05$; n.s., not significant.

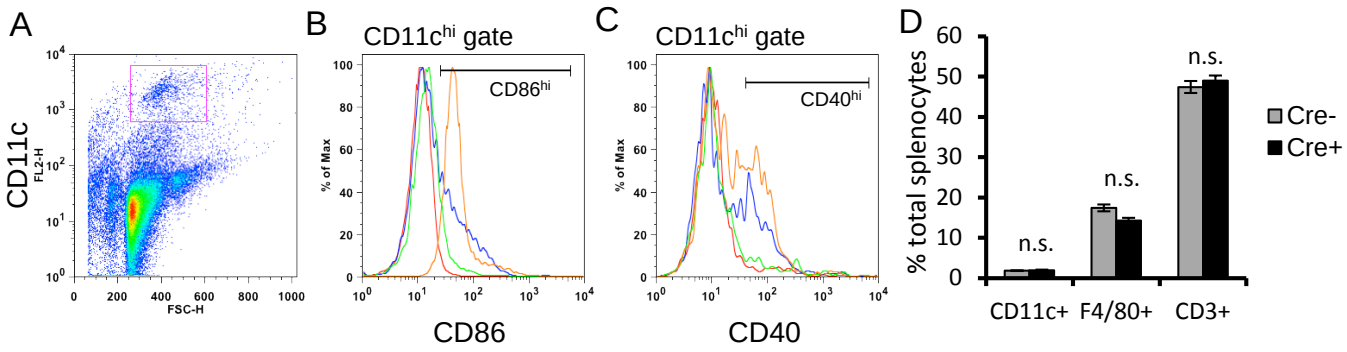

Supplementary Figure 2

Gating strategy for analysis of expression of CD11c, CD86, and CD40 in splenocytes of WD-fed *Cd11cCre^{+}Myd88$^{fl/fl}$* → *Ldlr$^{-/-}$* mice. For this figure and the following Supplementary figures, *Ldlr$^{-/-}$* mice transplanted with *Cd11cCre^{-}MyD88$^{fl/fl}$* (Cre-) or *Cd11cCre^{+}MyD88$^{fl/fl}$* (Cre+) bone marrow were fed the WD for 10 wks. **(A)** The boxed region represents CD11c^{hi} splenocytes. **(B-C)** Analysis of expression of CD86 and CD40 on CD11c^{hi}-gated cells in the following 4 groups of mice: WT control mice (red); WT mice injected with TLR9 activator CpG (orange); WD-fed Cre- mice (blue); and WD-fed Cre+ (green) mice. The CD86^{hi} and CD40^{hi} gates were based on expression levels of these maturation markers on splenic CD11c^{hi} cells isolated from mice injected with the CpG.(orange line). **(D)** Flow cytometric analysis of the relative distribution of DCs (CD11c+), macrophages (F4/80+), and T cells (CD3+) in the spleens of Cre- or Cre+ mice. n = 10 mice per group. *, $p<0.05$; n.s., no significant difference.

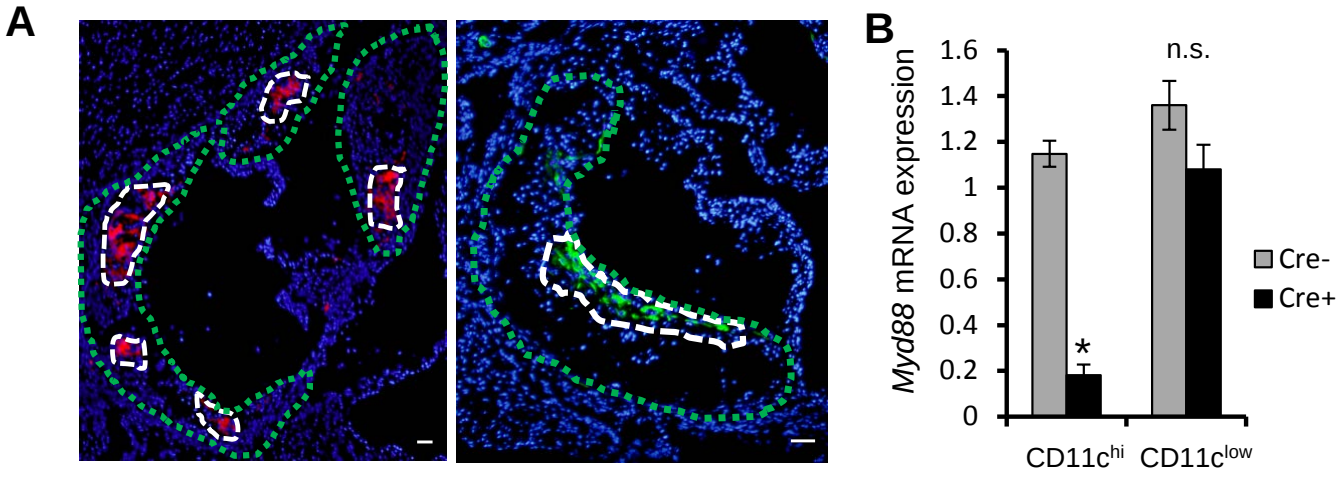

Supplementary Figure 3

***Myd88* mRNA is specifically deficient in the CD11c^{hi} regions of atherosclerotic lesions of WD-fed *Cd11cCre^{+}Myd88$^{fl/fl}$* → *Ldlr$^{-/-}$* mice. (A)** Identification of CD11c^{hi} (red staining, left panel) and sm-actin + regions (green staining, right panel) of atherosclerotic lesions by immunofluorescence microscopy. The green dotted lines demarcate the atherosclerotic intima. The region marked with dashed white line was captured as the CD11c^{hi} region (left panel) by LCM, and the remaining lesional areas were acquired as the CD11c^{low} region. In the right panel, the region marked with white dashed line was acquired as the sm-actin+ region. Bars, 10 μm. **(B)** *Myd88* mRNA levels were determined by RT-qPCR analysis of RNA captured from CD11c^{hi} and CD11c^{low} regions of the plaques of Cre- and Cre+ mice (n = 5 mice per group; *, $p<0.05$; n.s., no significant difference).

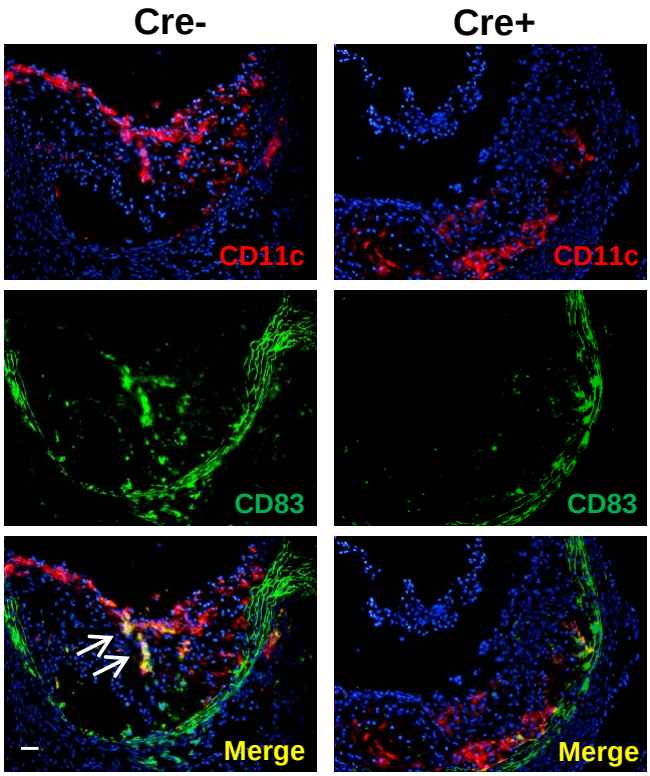

Supplementary Figure 4

Decrease in CD83+ mature DCs in aortic root lesions of WD-fed *Cd11cCre^{+}Myd88$^{fl/fl}$* → *Ldlr$^{-/-}$* mice.

Identification of CD11c (red) and CD83 (green) by immunofluorescence microscopy in lesions of Cre- and Cre+ mice. The nuclei are counterstained blue with Hoechst. *Arrows*: examples of cells with co-localization of CD11c and CD83. Bar, 10 µm.

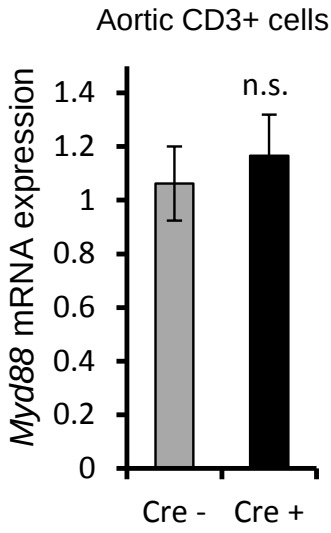

Supplementary Figure 5

***Myd88* expression in arterial wall CD3+ cells is similar in WD-fed *Cd11cCre*$^{-}$ *Myd88*$^{fl/fl}$ → *Ldlr*$^{-/-}$ and *Cd11cCre*$^{+}$*Myd88*$^{fl/fl}$ → *Ldlr*$^{-/-}$ mice.** *Myd88* mRNA was assayed in FACS-sorted CD3+ cells from the aortic arch and brachiocephalic artery of Cre- and Cre+ mice (n = 5 mice per group).

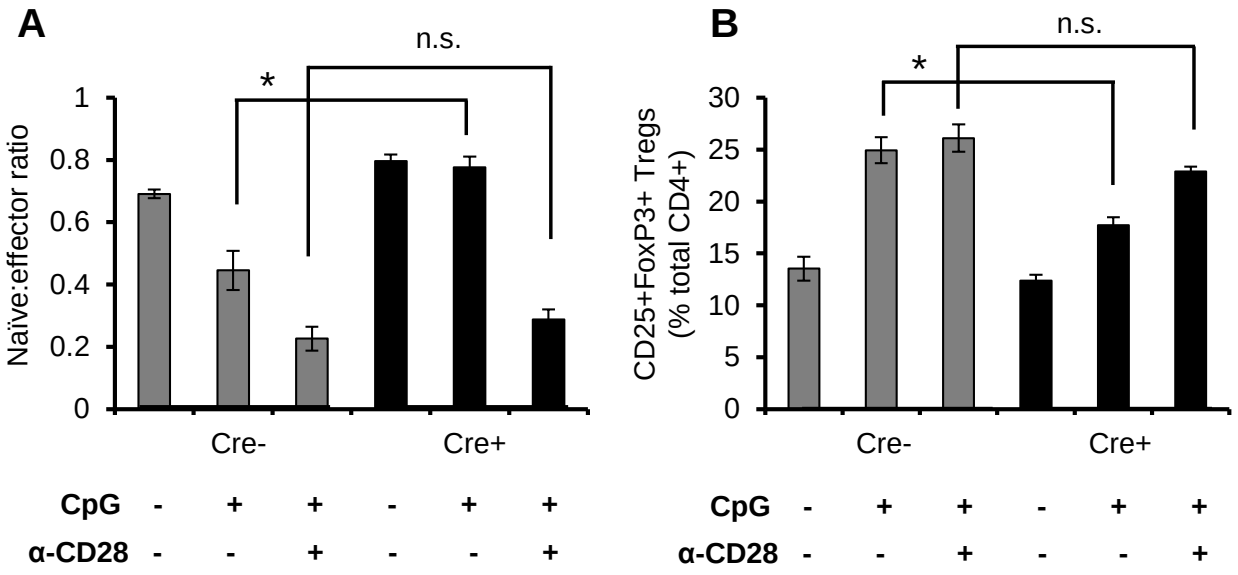

Supplementary Figure 6

Teff and Treg differentiation of naïve T cells incubated with MyD88-deficient DCs is defective and can be overcome by exogenous costimulation with α-CD28 antibody. Ova-loaded BMDCs from *Cd11cCre^{-}Myd88$^{fl/fl}$* and *Cd11cCre^{+}Myd88$^{fl/fl}$* mice were treated without or with CpG or anti-CD28 antibody (2 μg/ml) and then co-incubated for 72 h with naïve CD4+ T cells isolated from OT-II transgenic mice (>95% purity). The cells were then stained for CD4, CD44, CD62, CD25, and FoxP3 and analyzed by flow-cytometry. The bar graphs show the quantification of naïve (CD44^{low}CD62L^{hi}):effector (CD44^{hi}CD62L^{low}) T cell ratio **(A)** and Tregs **(B)** in the indicated groups. The data are representative of three independent experiments (*, $p<0.05$; n.s., no significant difference).

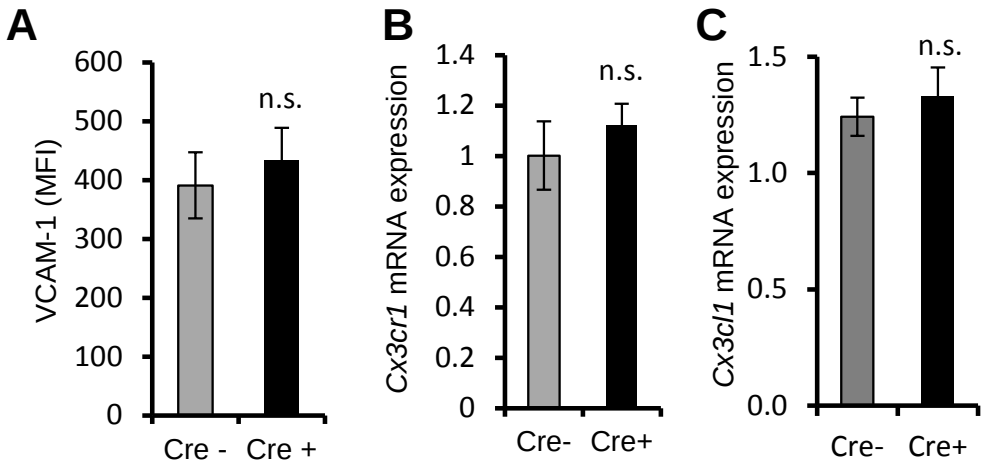

Supplementary Figure 7

VCAM-1, *Cx3cr1*, and *Cx3cl1* are similar in the lesions of WD-fed *Cd11cCre^{-}Myd88$^{fl/fl}$* → *Ldlr$^{-/-}$* and *Cd11cCre^{+}Myd88$^{fl/fl}$* → *Ldlr$^{-/-}$* mice.

(A) Quantification of VCAM-1 immunofluorescence on endothelial cells of atherosclerotic lesions in Cre- and Cre+ mice. **(B-C)** Quantification of *Cx3cr1* and *Cx3cl1* mRNA in CD11c^{low} regions of atherosclerotic lesions of Cre- and Cre+ mice. The data were normalized to *Gapdh* mRNA expression. n = 5 mice per group.

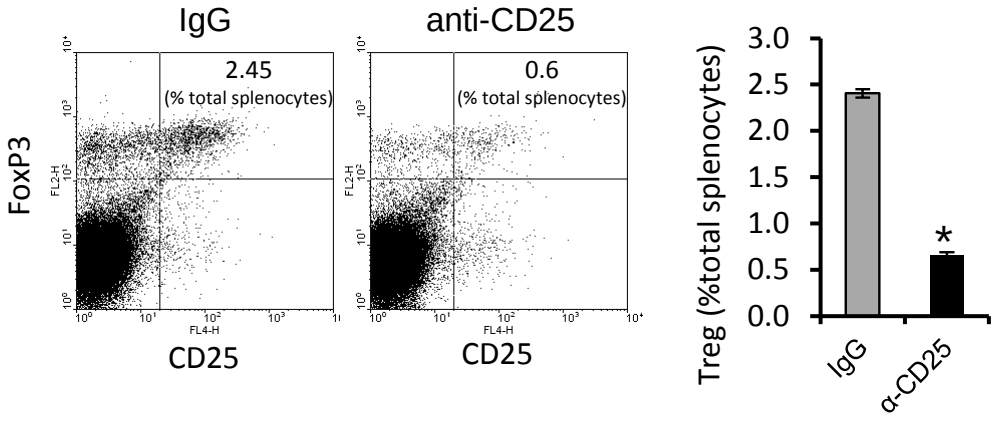

Supplementary Figure 8

Depletion of splenic Tregs in WD-fed *Cd11cCre^{-}Myd88$^{fl/fl}$* → *Ldlr$^{-/-}$* mice injected with anti-CD25 antibody. Representative dot plots demonstrating depletion of splenic Tregs (CD4+CD25+FoxP3+) 14 days post-injection of 25 µg anti-CD25 mAb vs. control IgG in Cre- mice. The bar graph shows quantification of the dot plot data. n = 5 mice per group.

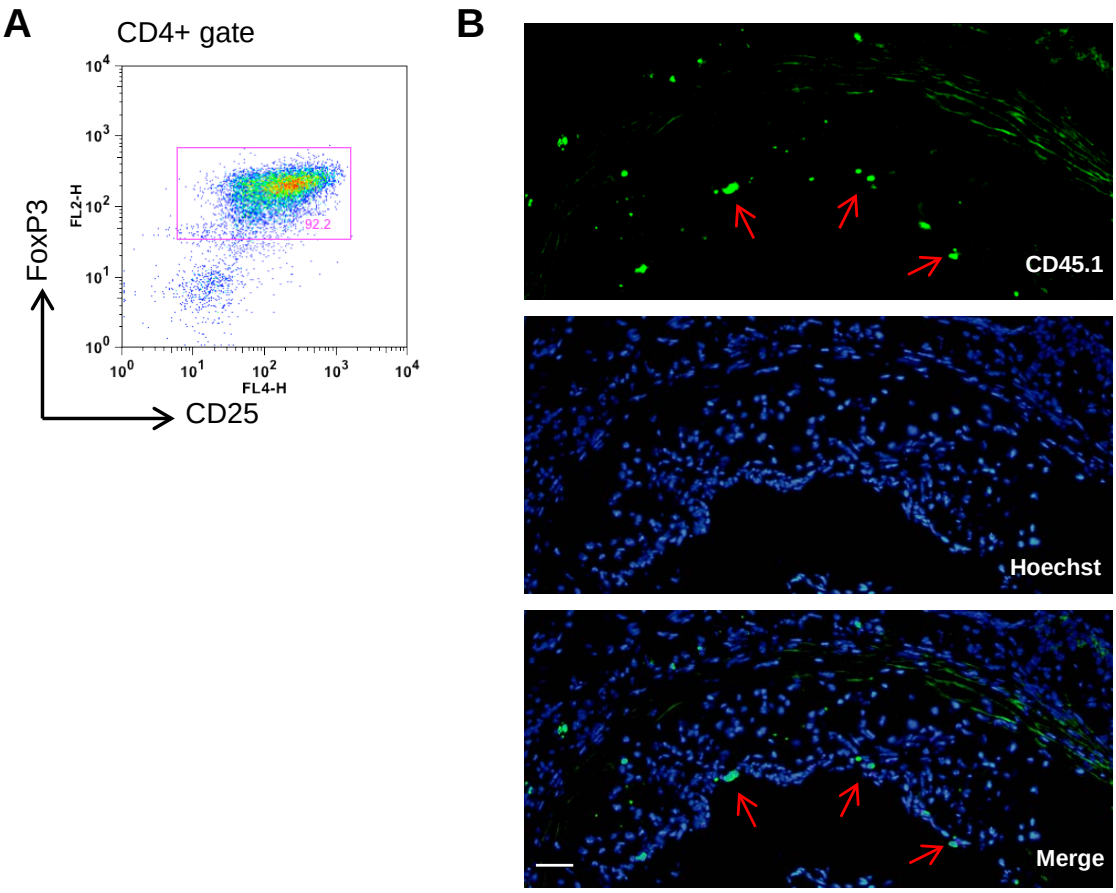

Supplementary Figure 9

FACS analysis of splenic Tregs from donor mice, and localization Tregs in lesions after adoptive transfer into WD-fed *Cd11cCre*$^{+}$*Myd88*$^{fl/fl}$ → *Ldlr*$^{-/-}$ mice

(A) Analysis of CD25 and FoxP3 expression in MACS-sorted CD4+CD25+ splenocytes. Note that >90% of sorted cells expressed the Treg specific marker FoxP3. **(B)** Fluorescence microscopic localization of CD45.1+ cells (green) in the atherosclerotic lesions of Cre+ mice that were adoptively transferred with Tregs isolated from the spleens of CD45.1+ *C57BL/6J* mice. Bar, 10 µm.

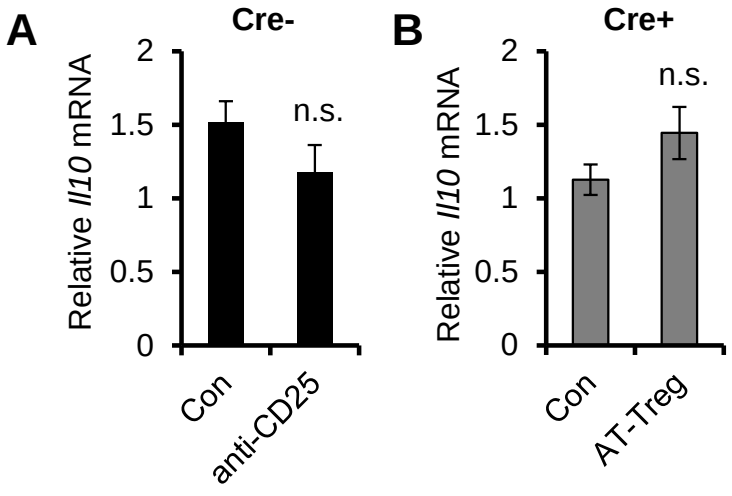

Supplementary Figure 10

***Il10* is similar in the lesions of WD-fed *Cd11cCre*$^{-}$ *Myd88*$^{fl/fl}$ → *LdIr*$^{-/-}$ *after Treg depletion* and *Cd11cCre*$^{+}$*Myd88*$^{fl/fl}$ → *LdIr*$^{-/-}$ mice after adoptive transfer of Tregs.** Analysis of *Il10* mRNA levels in CD11c^{hi} regions of atherosclerotic lesions of Cre- mice injected with IgG (Con) or anti-CD25 antibody **(A)** or Cre+ mice adoptively transferred with Tregs **(B)**. n = 5 mice per group; n.s., no significant difference.

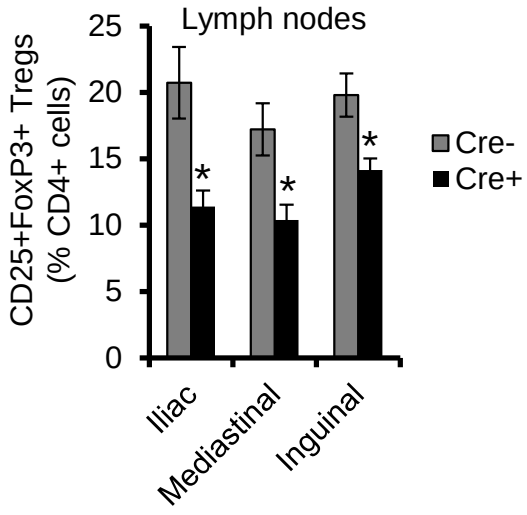

Supplementary Figure 11

Tregs are lower in the lymph nodes of *Cd11cCre^{+}Myd88$^{fl/fl}$ → Ldlr$^{-/-}$* mice. Flow cytometric quantification of (CD4+CD25+FoxP3+ Tregs as a percentage of CD4+ cells in the iliac, mediastinal, and inguinal lymph nodes of Cre- and Cre+ mice. n = 5 mice per group; *, $p<0.05$.

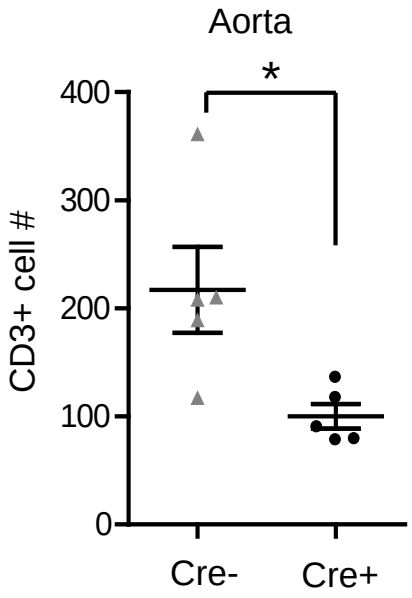

Supplementary Figure 12

CD3+ are lower in aortic extracts of *Cd11cCre^{+}Myd88$^{fl/fl}$ → Ldlr$^{-/-}$* mice. Flow cytometric quantification of total CD3+ cell numbers in aortic extracts of Cre- and Cre+ mice. n = 5 mice per group; *, $p<0.05$.